Experimental comparison of the impact of air-side particulate fouling on the thermo-hydraulic performance of microchannel and plate-fin heat exchangers

Abstract

In this study, the air-side pressure drop and heat transfer performance of plate-fin and microchannel coils were tested under clean and fouled conditions. The heat exchangers were tested with two different types of dust, ASHRAE dust and Arizona Road Test Dust. The ASHRAE dust was found to have a very significant impact on the pressure drop, increasing the air-side pressure drop of the microchannel heat exchanger over 200% for a dust injection of 267g. Fouling with Arizona Road Test Dust was not found to increase the air-side pressure drop but was found to decrease the heat transfer rate by more than 10%. In addition, from studies of the evolution of the air-side pressure drop during the fouling process, it is seen that microchannel coils with louvered fins with fin spacings below 2.0 mm were significantly more prone to fouling than heat exchangers with larger fin spacing.

Key words:
heat exchanger, fouling, pressure drop

1. Introduction

Over the last few decades there has been an increasing interest in air-side fouling of heat exchangers of many different constructions. From the numerous experimental studies carried out, a few overarching themes become clear. For one, fouling has a much more significant impact on air-side pressure drop than air-side heat transfer. In addition, the sensitivity of the heat exchanger to fouling is strongly dependent on the type of fouling as well as the particulars of the heat exchanger geometry.

1.1. Experimental and Modeling studies of Air-side fouling

Middis and Müller-Steinhagen (1990) studied asymptotic fouling resistance behavior of enhanced surface heat exchangers with particulate matter suspended in a liquid stream. They noted that the enhanced surfaces with more stagnation areas were more prone to foul.

Zhang et al. (1992) investigated the addition of spoilers upstream of heat exchangers in order to introduce turbulence and decrease the deposition of particulate matter. They found that angling the spoilers at an angle of 30 degrees with respect to the incoming air stream resulted in the best performance.

Kaiser et al. (2002) studied the deposition of an analog of dryer lint to a cooled probe. No heat transfer or pressure drop measurements were made, but a strong sensitivity to air humidity and particle concentration was found.

One of the only studies which attempted to model particle deposition to a surface was the study carried out by Siegel (2003). This study focused on an understanding of the competing physical processes which result in particulate deposition on the surface. It was also found from this study that the impacts of fouling is a decrease in the air flow-rate of 5-6% and a decrease in system efficiency of 2-4%.

Ahn et al. (2003) collected field-installed fouled evaporators and tested them in a laboratory facility. For evaporators installed in the field for up to 7 years, the air-side pressure drop increased up to 45% over the duration of the tests. In addition, the heat transfer decreased by up to 14%. It is not clear what size heat exchangers were used, nor the total amount of dust on the heat exchangers.

Lankinen et al. (2003) investigated the impact of air-side fouling on the compact heat exchangers with needle-fins using ASHRAE standard dust similar to that under investigation here. They found increases in air-side pressure drop up to 200% and decreases in the overall heat transfer coefficient of 8% to 18% with the injection of 8.3 kg of dust into the air stream. Neither frontal area of the heat exchanger nor fin geometry was given.

Pak et al. (2005) fouled one- and two-row HVAC condenser coils. They found that the two-row coils experienced an increase in air-side pressure drop up to 31%, while the maximum increase in air-side pressure drop for two-row coils was 37%. The heat transfer rate of the one-row coils decreased up to 12%, and that of the two-row coils decreased up to 5%. 300g of ASHRAE dust were used to foul the coil of frontal area 0.44 m^2.

Mason (2006) fouled a compact heat exchanger with straight and herringbone fins with sawdust particles. This study demonstrated that the smaller the fin spacing, the greater the increase in pressure drop, for both fin styles. This study also demonstrated the existence of two fouling regimes, firstly nucleation fouling where primarily large particles deposit. After passing a critical change over

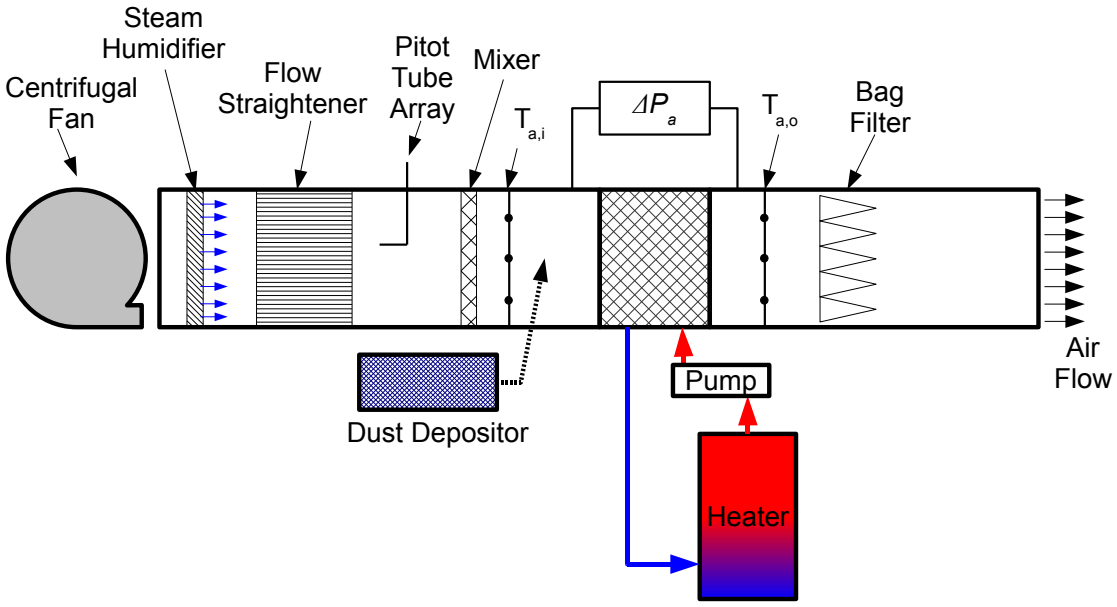

Figure 1: Schematic of Wind Tunnel used for heat exchanger testing

point, the pressure drop rapidly increases in the bulk fouling regime where a much higher percentage of the particles adhere to the fins. Mason also found that most of the fouling adhered to the front face of the coil.

Haghighi-Khoshkhoo and McCluskey (2007) also investigated fouling heat exchangers with sawdust. They found a particle size which would always pass through the heat exchanger which was dependent on heat exchanger geometry. Neither the tube wall temperature nor fouling injection rate was found to have any impact on the rate of fouling deposition. The fouling was also found to occur on the front face of coil, resulting in little to no increase in heat transfer resistance, but significant increase in air-side pressure drop. Significant absolute increases in air-side pressure drop are shown, but the baseline air-side pressure drop is not given.

Yang et al. (2007b) carried out experiments on the fouling performance of HVAC evaporators with upstream filters. When no filters were utilized upstream of the heat exchanger, the pressure drop always increased, up to an increase of 200% from the unfouled condition. Without filters, the air-side heat transfer also decreased, up to 14% for coils with 2 passes. When filters were used, it was found that slight improvements in heat transfer performance were realized for heat exchangers 8 rows deep due to fin surface enhancement.

1.2. System-level impact

Condensers and evaporators do not operate individually, but are typically integrated into larger HVAC systems. As a result, it is critical to investigate the impact of fouling at the system level.

Yang et al. (2007a) investigated the system-level impacts of the heat exchanger fouling results presented in Yang et al. (2007b), from which they found that the impact of the fouling was a decrease in system efficiency of up to 10%.

Krafthefer (1986) found that the pressure drop of fouled coils can cause a doubling of the air-side pressure drop after 5-7 years. With a doubling of the air-side pressure drop over the evaporator, the efficiency of the heat pump decreased by 18%.

Breuker (1998) investigated the impacts of various different faults on rooftop air conditioning units. With a 56% blockage of the front area of the condenser, the net result was a decrease in cooling capacity of 10.9% and a 17.9% decrease in the system efficiency due to the increase in condensing pressure.

2. Testing Procedure

2.1. Heat Exchangers Tested

Three different heat exchangers were tested in the current study. All of the heat exchangers were designed as refrigerant condensers, but there are some significant differences in construction between the heat exchangers. Heat exchanger A is a plate-fin style condenser. Heat exchangers B and C are both Microchannel condensers with louvered fins. Measurements of heat transfer performance and air-side pressure drop of heat exchangers A and B were made with under clean and fouled conditions, the details of which are presented in section 4. After conducting the full battery of thermo-hydraulic tests on heat exchangers A and B, subsequent air-side pressure drop measurements were made on heat exchangers A, B & C during the course of the fouling process in order to quantify the propensity of a given heat exchanger to foul. The heat exchangers which were tested in this study are shown in Table 1.

Table 1: Geometry of heat exchangers from this study

Key	Type	Frontal Area	Fin Spacing	Fin Type
A	Plate-Fin heat exchanger	40x50 cm	2.0 mm	Wavy
B	Microchannel HX	40x50 cm	1.3 mm	Louvered
C	Microchannel HX	40x50 cm	1.1 mm	Louvered

2.2. Test Facility

All three of the heat exchangers were installed in a forced flow wind tunnel with nominal internal cross section of 60x60cm. Since all the heat exchangers tested in this study have 40x50cm frontal area, they were installed in reducing sections to permit their use in the wind tunnel.

The heat exchanger testing facility operates by passing relatively warm water through the coil and cooler air over the tubes and fins of the heat exchanger in order to provide the cooling effect. The warm water is provided by a water loop with a controllable water heater in order to set the water inlet temperature as seen in Figure 1. The balance of the heat provided by the variable-power heater and the heat removed by the heat exchanger allows for control of the water inlet temperature.

On the air side, conditioned air from the laboratory is drawn into the blower where it is accelerated to the desired duct air velocity under variable frequency control of the fan speed. In order to eliminate variation in supply air temperature due to variation in laboratory air temperature, the air is always heated up to above the ambient temperature. Steam valves installed after the blower humidify the air if necessary by adding moisture to the air stream. After the flow has been appropriately conditioned, it passes through a section of flow straighteners to ensure that the flow is aligned with the duct. Then the air flow velocity is measured with a pitot-tube array. Prior investigators found the velocity profile over the duct cross-section to be very uniform. A mixing section is subsequently used to thoroughly mix the air flow. After mixing, dust is injected into the air stream as described in section 2.4, the air passes through the heat exchanger, and the air is filtered through bag filters prior to exhausting outdoors.

The air-side pressure drop of the heat exchanger is measured based on the wall pressures upstream and downstream of the heat exchanger. At a cross-section, the pressure taps are connected to average the pressure over the four walls of the wind tunnel. The upstream and downstream averaged pressure taps are then connected to a differential pressure sensor with full scale range of 249.1 Pa (1.0" H_2O) and uncertainty of 2.49 Pa (1% of full scale) to measure the air-side pressure drop over the heat exchanger. For the final segment of the fouling process for heat exchanger C, a differential pressure sensor with full scale range of 2491 Pa (10" H_2O) was used to measure air-side pressure drop since the air-side pressure drop exceeded 249.1 Pa. The pressure drop of the pitot tube array is measured with a differential pressure sensor with full scale range of 24.91 Pa (0.1" H_2O) and uncertainty of 0.062 Pa (0.25% of full scale).

The temperatures of the air stream upstream and downstream of the heat exchanger were measured with 3x3 grids of K-type thermocouples with estimated uncertainty of 0.5°C. The mean temperature over each grid was used in further calculations of enthalpies. The mean air temperature measured at the upstream temperature grid is used in the calculation of the heat exchanger inlet air density. The relative humidity was also measured upstream and downstream of the heat exchanger with uncertainty of 1% of the measurement. Over all the tests carried out, the maximum difference between the upstream and downstream measurements of humidity ratio was 4.0 %, and most points were within 2.0 %. Since there is no condensation or evaporation of water in the heat exchanger, the humidity ratio should be constant over the heat exchanger. The low difference in humidity ratio suggests that the dry bulb temperatures and relative humidities were properly measured.

For the water loop, heat exchanger inlet and outlet temperatures were measured with T-type thermocouples with uncertainty of 0.5°C, and the water mass flow rate was measured with a Coriolis mass flow meter with uncertainty of 0.4%.

2.3. Testing points

Heat exchangers A and B were tested at a wide range of state points in clean and fouled conditions. For heat exchangers A and B, the water and air mass flow rates both varied, though the ratio of the air to water mass flow rates was held nominally constant at 4.184 in order to achieve similar temperature differences for both air and water streams when passing through the heat exchanger. The testing points of Table 2 were used for heat exchangers A and B under clean and fouled conditions.

Table 2: Nominal Testing Points

Parameter	Value
$T_{a,i}$ [°C]	25
$T_{w,i}$ [°C]	42
ϕ_i [%]	40
$\dot{m}_w$ [kg/s]	0.103, 0.132, 0.153, 0.179, 0.208
$\dot{m}_a$ [kg/s]	$4.184 \cdot \dot{m}_w$

2.4. Dust and Dust injection

Two different types of dust were tested with the heat exchangers. The first style of dust is ASHRAE dust which

is standardized dust typically used for testing of air filters, as in ASHRAE Standard 52.1. The distinguishing characteristic of this dust is the high volumetric fraction of cotton lint. The mass composition of this dust is 72% A2 fine Arizona Test Dust, 23% carbon black powder, and 5% second cut cotton linters milled in a Wiley Mill fitted with a 4 mm screen. While this dust is a good analog for residential dust, it can also approximate exterior dust for condensers installed near fouling sources. Field installed condensers have demonstrated high levels of fibrous loading, as seen in Figure 2. This is particularly a problem near agricultural installations, as noted by Mason (2006).

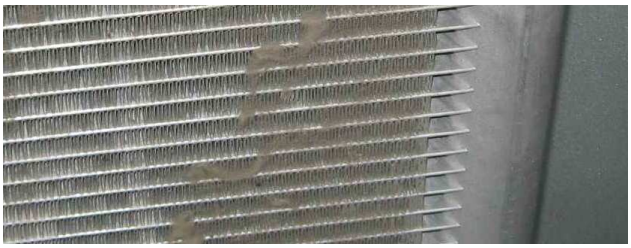

Figure 2: Field installed heat exchanger demonstrating large amount of fibrous loading

In areas with little fibrous content in the fouling matter, Arizona Road Test Dust may be a better analog. Arizona Road Test Dust is a component of the ASHRAE test dust, but can also be obtained individually. Arizona Road Test Dust is available in a range of particle size distributions, and A2 Fine Arizona Road Test was selected. The mass composition of this dust is approximately 72% SiO_2, 12.5% Al_2O_3, all other components being less than 3% each. Figure 3 shows the particle size distribution of the A2 Fine Test Dust. 80% of the particles are between 1 and 30 μm in diameter.

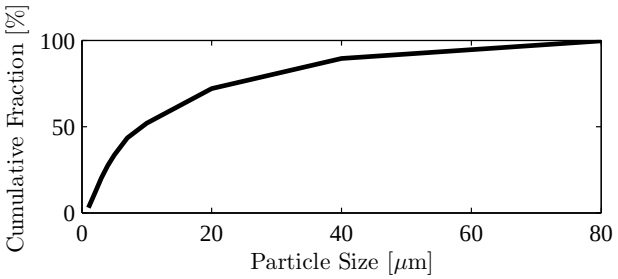

Figure 3: Particle size distribution of A2 Arizona Road Test Dust

In order to foul the heat exchanger, batches of approximately 33.3 g of dust (either ASHRAE or Arizona) are massed on a scale and spread out on the feeding tray of the dust depositor shown in Figure 4. A gear drive slowly moves the dust tray towards the aspirator head, and the metering wheel rotates in sync with the tray in order to control the rate of dust being drawn into the aspirator head. The rate of dust injection is therefore controlled by the amount of dust added to each tray. The rate of feed of the dust injector is approximately one tray every 20 minutes, for a rate of dust injection of 100 g of dust per hour.

During the fouling process, the duct air velocity was held constant at 1.5 m/s, for a coil face velocity of 2.8 m/s. In order to maintain the duct air velocity, the fan speed was manually increased throughout the fouling process. Lower air velocities could not be used repeatably since the dust falls out of suspension for lower air velocities.

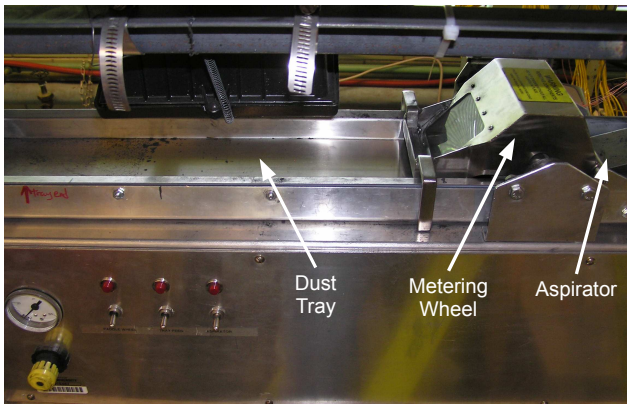

Figure 4: Dust Injector

3. Data Analysis

The air velocity in the duct is measured with pitot tubes and is calculated from the application of Bernoulli's equation along a stream line, which yields

$$u_{duct} = \sqrt{\frac{2\Delta p_{pitot}}{\rho_{duct}}} \tag{1}$$

where the air density ρ_{duct} is calculated based on the temperature at the pitot tubes and the ambient pressure. From the air velocity it is therefore possible to calculate the air mass flow rate, given by

$$\dot{m}_a = u_{duct}\rho_{duct}A_{duct} \tag{2}$$

where the actual duct cross sectional area A_{duct} is (0.372 m^2). For heat exchangers A and B, the coil frontal area is less than the duct cross-sectional area, and the face velocity can be calculated from

$$u_{face} = \frac{A_{duct}}{A_{face}}u_{duct} \tag{3}$$

The air-side heat transfer is therefore given by

$$q_a = \dot{m}_a(h_{a,o} - h_{a,i}) \tag{4}$$

where $h_{a,o}$ and $h_{a,i}$ are humid air mixture enthalpies. The water-side heat transfer is given by

$$q_w = \dot{m}_w c_{p,w}(T_{w,i} - T_{w,o}) \tag{5}$$

The heat exchanger is a cross-flow type heat exchanger. For each test, the inlet temperature difference between the water and air inlet streams (ΔT_1) was held at a nominal value of 17°C, but to correct for slight differences in inlet temperatures, the overall heat transfer of the coil is presented as $q_w/\Delta T_1$. The water-side heat transfer measurement is used here rather than the air-side heat transfer since the measurement uncertainty is lower. In addition, the water-side heat transfer measurement devices are more robust and less sensitive to outside perturbances.

Since the ambient pressure in the lab can vary somewhat over the year, it is necessary to correct the air-side pressure drop for the ambient pressure. In general the air side pressure drop between two plates (like the fins) is proportional to the air density. Thus a corrected air-side pressure drop can be based on a standard density of air of 1.2 kg/m^3, and expressed as

$$\Delta p_{a,corrected} = \frac{1.2 \text{ kg/m}^3}{\rho_{a,measured}} \Delta p_{a,measured} \quad (6)$$

The corrected air-side pressure drop is generally close to the measured pressure drop since the air density in the laboratory was typically near 1.17 kg/m^3.

3.1. Measurement Uncertainty Propagation

Figure 5 shows the uncertainty propagations of the calculated and measured values as a function of the air mass flow rate for the clean state for heat exchanger B. As all the thermo-hydraulic tests were carried out at the same state points, these can be taken as representative uncertainties for all the thermo-hydraulic tests conducted.

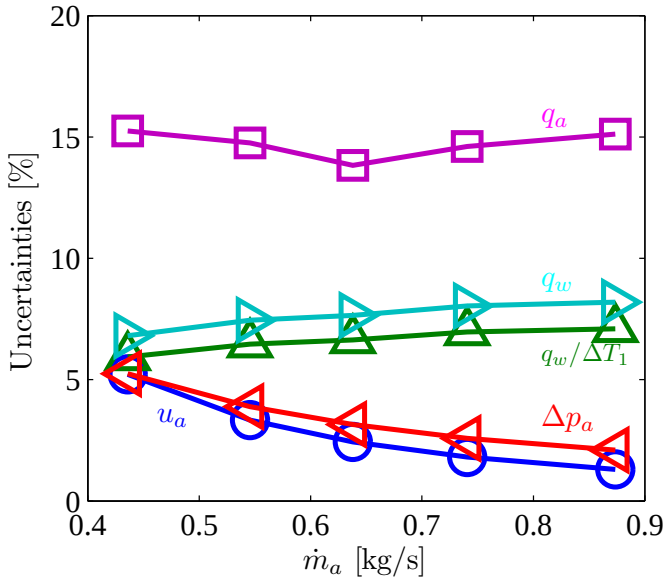

Figure 5: Uncertainties of measured values

4. Results

4.1. Thermo-hydraulic tests with fouling

As described above, tests were carried out with heat exchangers A & B under clean and fouled conditions. Figures 6 and 7 present results of air-side pressure drop and heat transfer for heat exchanger A. Considering first the clean data points, it is clear that as the flow rates of water and air increase, the overall heat transfer also increases. This is because the higher flow rates result in improved air- and water-side heat transfer coefficients, which ultimately result in improved heat transfer. As the mass flow rate of air increases, the face velocity increases as well, resulting in higher pressure drops over the coil. These clean heat transfer and pressure drop results are consistent with fundamental principles of heat transfer.

Figure 6 shows that the impacts of fouling with ASHRAE dust and Arizona dust on air-side pressure drop are significantly different. With the injection of 500g of Arizona dust, there is no measureable increase in air-side pressure drop. On the other hand, when 400g of ASHRAE dust is injected into the air stream, the air-side pressure drop increases 55.6% from the clean pressure drop for a duct air velocity of 2.0 m/s. On an absolute basis, the increase in air-side pressure drop due to fouling increases as the flows of air and water are increased.

Figure 7 shows that the impact of fouling with either ASHRAE dust or Arizona dust on heat transfer for heat exchanger A is not very significant, though the net impact of fouling is to decrease the heat transfer rate. At the highest flow rates of water and air, fouling results in decreases in heat transfer of 2.9% and 5.3% for ASHRAE and Arizona dusts respectively.

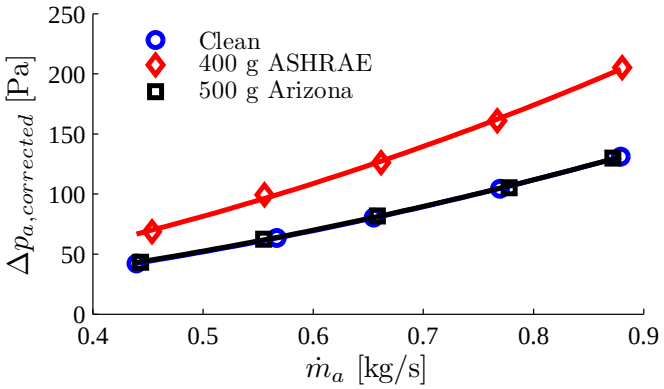

Figure 6: Pressure drop of HXA with fouling

In general, the microchannel-style heat exchanger B is significantly more sensitive to fouling than the plate-fin heat exchanger A. With the injection of only 135g of ASHRAE dust, there is a 45.5% increase in air-side pressure drop at a duct air velocity of 2.0 m/s. For the Arizona dust, there is a small overall decrease in air-side pressure drop with the injection of 500g of dust. This is believed

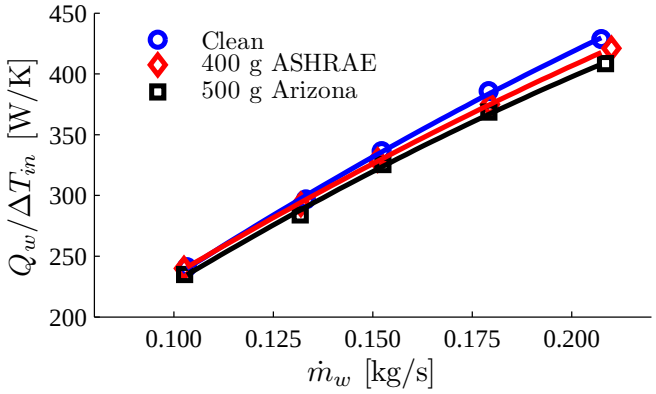

Figure 7: Heat transfer of HXA with fouling

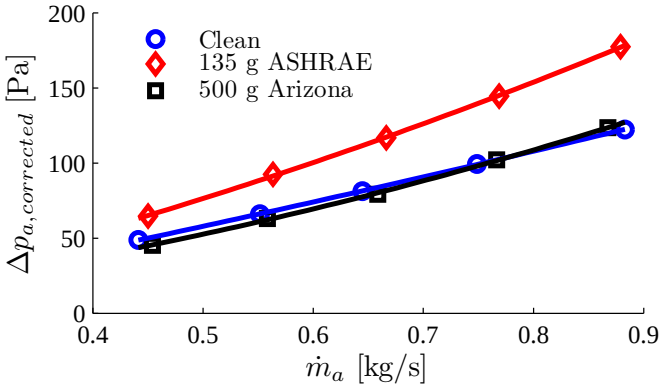

Figure 8: Pressure drop of HXB with fouling

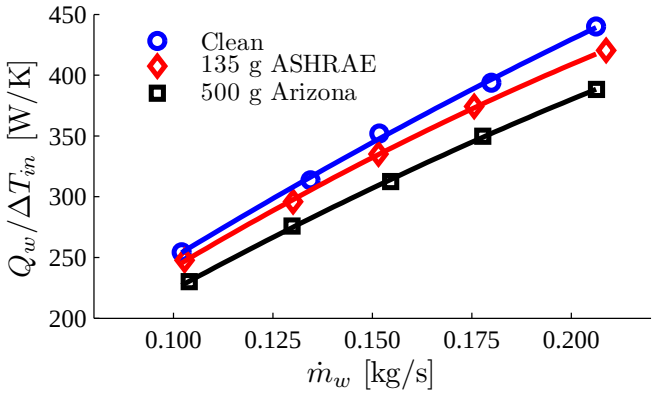

Figure 9: Heat transfer of HXB with fouling

to be due to the Arizona dust blocking up the louvers, resulting in a higher percentage of duct-directed flow straight through the heat exchanger rather than the louver-directed flow. Since the straight-through path is less circuitous, a lower pressure drop would be experienced.

At the highest air and water flow rates, the injection of 135g of ASHRAE dust results in up to a 5.2% reduction in heat transfer, while the Arizona dust results in up to 13.1% reduction in heat transfer. This significant reduction in heat transfer with the Arizona test dust is believed to be due to two factors - the louver blockage as described earlier as well as the blanket of low thermal-conductivity dust covering the extended surfaces. The macro photographs in the next section will help to visually explain these results.

For the ASHRAE dust, the fouling of the microchannel heat exchanger (B) with 135g of dust and the plate-fin heat exchanger (A) with 400g of dust result in similar decreases in heat transfer and increases of air-side pressure drop. Thus qualitatively it is possible to state that the microchannel heat exchanger is more strongly impacted by the fouling with ASHRAE dust. Similarly, fouling both heat exchangers A and B with 500g of Arizona dust results in a larger decrease in heat transfer for the microchannel heat exchanger (B). The microchannel design is more reliant on surface enhancement in order to decrease the air-side thermal resistance, and more sensitive to pertubations of the flow patterns within the heat exchanger.

4.2. Fouling Phenomena

The differences in fouling behavior between ASHRAE and Arizona Road Test Dust for heat exchangers A and B can be better understood by considering macro photographs of the heat exchangers with and without fouling. Figure 10 shows photographs of the heat exchangers under the fouling levels investigated in the thermo-hydraulic tests. For the ASHRAE dust, the particulate matter of the dust tends to build up on the front face of the coil for both heat exchangers A and B, forming a mat. At the extreme case, as in heat exchanger C fouled with 267g of ASHRAE dust, the coil is nearly entirely blocked. The same behavior is seen for heat exchanger B (microchannel) under similar levels of fouling.

For the Arizona Road Test Dust, the particulate matter coats all surfaces of the heat exchanger enhanced surface, particularly the stagnation regions. The thermal conductivity of the Arizona test dust is lower than that of the fin material, resulting in the significant decrease in heat transfer. The relatively thin film of particulate matter results in an insignificant increase in air-side pressure drop due to a negligible blockage of the frontal area.

4.3. Fouling Evolution

Mason et al. (2006) previously investigated the air-side particulate fouling behavior of a heat exchanger; the results of one test are shown in Figure 11 for reference. Here it is possible to clearly see two phases with very different behavior. At the beginning of the test, a relatively small amount of particulate matter adheres to the coil in the so called nucleation regime, resulting in a relatively slow linear growth of the air-side pressure drop. After a critical point, nearly all the particulate matter adheres to the heat exchanger; this is called the bulk fouling regime, and the air-side pressure drop increases very rapidly.

Similar tests were carried out on heat exchangers A, B, and C with ASHRAE dust. Qualitatively similar pressure

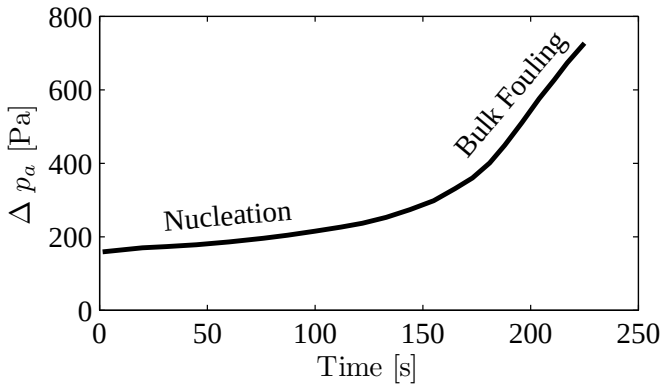

Figure 11: Evolution of the air-side pressure drop during the fouling process (Adapted from Mason et al.(2006))

drop evolutions were seen, though heat exchanger B fouls more strongly. Figure 12 shows the fouling evolutions of the three heat exchangers tested here compared with other heat exchangers from literature. The amount of fouling injected is divided by the frontal area of the heat exchanger in order to provide a fair comparison among the heat exchanger of different sizes. The heat exchangers selected from literature were those with sufficiently well characterized tests, louvered fins, and heat exchanger fouling conducted with ASHRAE dust in order to make the most fair comparison between studies. The specifications of the heat exchangers from literature are summarized in Table 3.

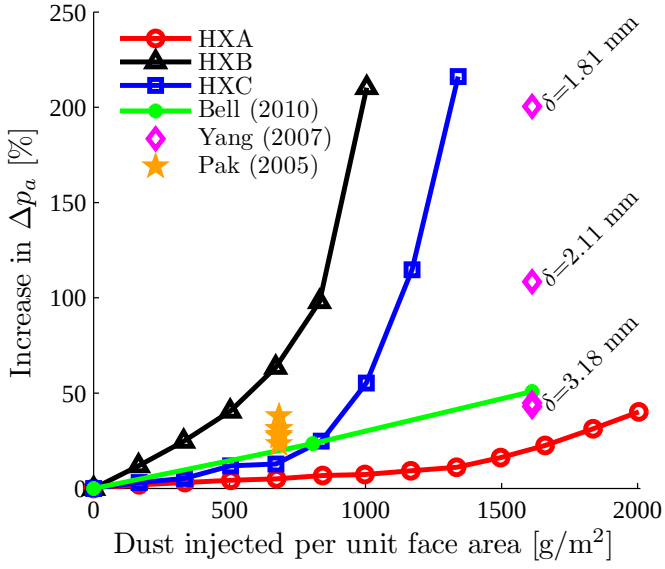

Figure 12: Literature survey of impact of ASHRAE Dust Fouling

In general, these results suggest that as the amount of injected dust is increased, the air-side pressure drop will increase monotonically. The significant difference in air-side pressure drop between the results of Yang et al. and Pak et al. can be reconciled by considering the fouling regime. While the results from Pak et al. are believed to be from the nucleation regime, the results from Yang et al. appear to be from the bulk fouling regime.

All the heat exchangers investigated in this study exhibit the same two-regime fouling process. Both heat exchangers A and C begin with a slow rate of increase of air-side pressure drop with fouling, hit a critical fouling amount and begin to foul much more quickly. For the plate-fin heat exchanger (A), the rate of bulk-fouling is still fairly low. In contrast, the microchannel heat exchangers (B and C) exhibit very high rates of fouling in the bulk-fouling regime. In the bulk-fouling regime the the microchannel heat exchangers (B and C) behave more like filters than heat exchangers. For a clean heat exchanger B, the injection of only 33.1g of dust results in an increase of pressure drop of 10%. Heat exchanger B could be more fairly described as having bulk-fouling and extreme bulk-fouling regimes.

For the louver-finned heat exchangers, as the fin spacing decreases, the propensity to foul increases, which is consistent with the results presented in Mason et al. (2006). In order to compare the bulk-fouling behavior of the louvered fin heat exchangers, the pressure drops for heat exchangers B and C were linearly extrapolated to the fouling amount of Bell et al. (2010) and Yang et al. (2007b) of 1612.5 g/m^2 ASHRAE dust per unit heat exchanger frontal area. Figure 13 shows the sensitivity to the fin spacing of the fouled pressure drop of the louvered finned heat exchangers in the bulk fouling regime. A regression was empirically fit to the data in order to approximate the shape of the curve.

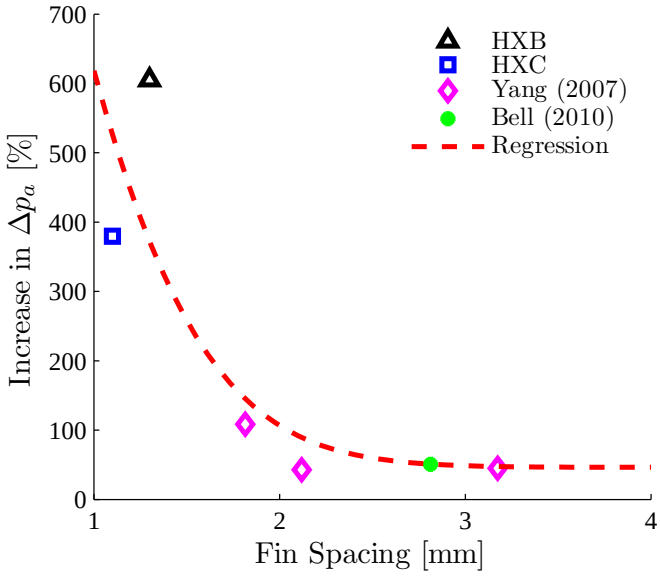

Figure 13: Increase in air-side pressure drop as a function of fin spacing for louvered fins with 1612.5 g/m^2 ASHRAE dust injected

Another major factor impacting fouling behavior is the louver geometry. Considering the air-side pressure drops for the results from Pak et al. (2005), Bell et al. (2010) and heat exchangers B and C, it is clear that the fin lou-

Table 3: Heat Exchangers from literature fouled with ASHRAE Test Dust

Author	Name	$A_{frontal}$	Fin Type	δ [mm]
Pak et al.	HX01	488 x 902 mm	Plain fins	1.15
Pak et al.	HX02	488 x 902 mm	Louvered fins	1.15
Pak et al.	HX04	488 x 902 mm	One-by-one louvered fins	1.15
Pak et al.	HX05	488 x 902 mm	Continuous louvered fins	1.15
Yang et al.	HX8L	610 x 610 mm	Louvered wavy fins	3.17
Yang et al.	HX4L	610 x 610 mm	Louvered wavy fins	2.19
Yang et al.	HX2L	610 x 610 mm	Louvered wavy fins	1.81
Bell et al.	N/A	610 x 610 mm	Louvered fins	2.81

vering plays a large role. All these heat exchangers have the same amount of dust injected per face area (about 600 g/m^2), all have louvered fins, and all have similar louver fin spacing. Thus the only variable is the details of the fin louvers. While details are not available on the louvering of the heat exchangers of Pak et al. or Bell et al., some differences can be noted between heat exchangers B and C. Heat exchanger B is more aggressively louvered; that is, the louvers protrude more significantly into the air stream, providing for more "scooping" of the air, resulting in a smaller effective fin spacing. In addition, the louvers of heat exchanger B begin at nearly the leading edge, while the louvers of heat exchanger C begin about 4.7mm from the front face of the heat exchanger. A thorough understanding of the impact of louver geometry on fouling behavior is critical but is beyond the scope of this paper.

5. Conclusions

Thermo-hydraulic tests were carried out on ASHRAE and Arizona dust were tested with plate-fin and microchannel heat exchangers. In addition, the pressure drop of the heat exchangers were measured during the fouling process. From these tests, the following conclusions are possible:

- The ASHRAE dust results in a much larger increase in air-side pressure drop than the Arizona dust.
- Arizona dust results in a larger decrease in heat transfer
- The microchannel coil tested was much more sensitive to fouling by either Arizona or ASHRAE dust than the plate-fin heat exchanger
- From the comparison with data in literature, it appears fin spacing below about 2.0 mm for louvered fins results in an extreme sensitivity to particulate fouling in the bulk fouling regime.

References

Ahn, Y.-C., Cho, J.-M., Shin, H.-S., Hwang, Y.-J., Lee, C.-G., Lee, J.-K., Lee, H.-U., Kang, T.-W., Sep. 2003. An experimental study of the air-side particulate fouling in fin-and-tube heat exchangers of air conditioners. Korean Journal of Chemical Engineering 20 (5), 873–877.

Bell, I., Groll, E., König, H., 2010. Experimental analysis of the effects of particulate fouling on heat exchanger heat transfer and air side pressure drop for a hybrid dry cooler. Heat Transfer Engineering In Press.

Breuker, M. S., Braun, J. E., 1998. Common faults and their impacts for rooftop air conditioners. HVAC and R Research 4 (3), 303 – 317.

Haghighi-Khoshkhoo, R., McCluskey, F. M. J., 2007. Air-side fouling of compact heat exchangers for discrete particle size ranges. Heat Transfer Engineering 28, 58–64(7).

Kaiser, S., Antonijevic, D., Tsotsas, E., 2002. Formation of fouling layers on a heat exchanger element exposed to warm, humid and solid loaded air streams. Experimental Thermal and Fluid Science 26 (2-4), 291 – 297.

Krafthefer, B., Bonne, U., 1986. Energy use implications of methods to maintain heat exchanger coil cleanliness. In: ASHRAE Transactions. Vol. 92. San Francisco, CA, USA, pp. 420 – 431.

Lankinen, R., Suihkonen, J., Sarkomaa, P., 2003. The effect of air side fouling on thermal-hydraulic characteristics of a compact heat exchanger. International Journal of Energy Research 27 (4), 349–361.

Mason, D., Heikal, M., Douch, N., 2006. Air side fouling of compact heat exchangers. International Journal of Heat Exchangers 1, 1–14.

Middis, J., Muller-Steinhagen, H., 1990. Particulate fouling in heat exchangers with enhanced surfaces. In: CHEMECA '90, Australasian Chemical Engineering Conference. Auckland, NZ, pp. 1053 – 1060.

Pak, B. C., Groll, E. A., Braun, J. E., 2005. Impact of fouling and cleaning on plate fin and spine fin heat exchanger performance. In: ASHRAE Transactions. Vol. 111 PART 1. Orlando, FL, United states, pp. 496 – 504.

Siegel, J. A., Nazaroff, W. W., 2003. Predicting particle deposition on hvac heat exchangers. Atmospheric Environment 37 (39-40), 5587 – 5596.

Yang, L., Braun, J. E., Groll, E. A., 2007a. The impact of evaporator fouling and filtration on the performance of packaged air conditioners. International Journal of Refrigeration 30 (3), 506 – 514.

Yang, L., Braun, J. E., Groll, E. A., 2007b. The impact of fouling on the performance of filter-evaporator combinations. International Journal of Refrigeration 30 (3), 489 – 498.

Zhang, G., Bott, T., Bemrose, C., 1992. Reducing particle deposition in air-cooled heat exchangers. Heat Transfer Engineering 13 (2), 81 – 87.

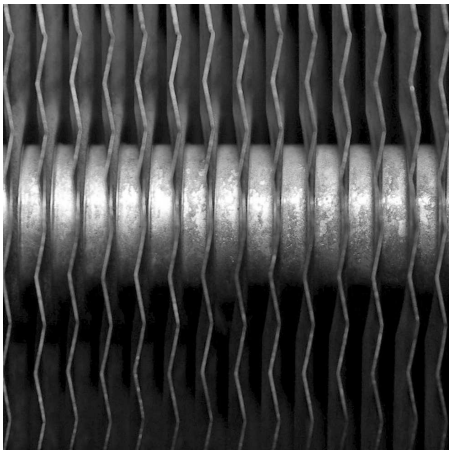

Heat Exchanger A Clean

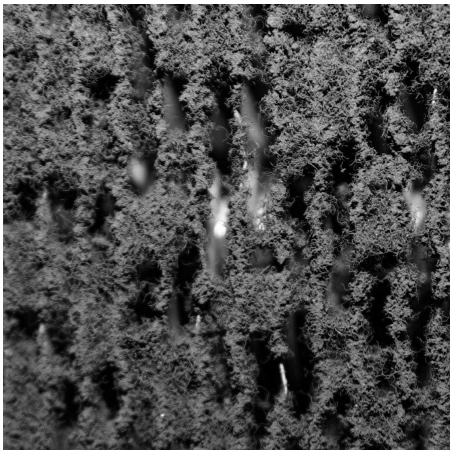

Heat Exchanger A Fouled with 400 g ASHRAE Test Dust

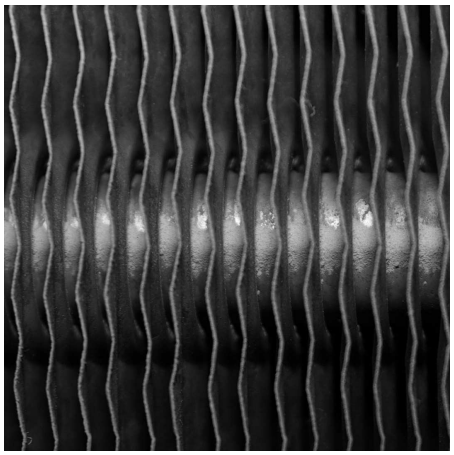

Heat Exchanger A Fouled with 500 g Arizona Road Test Dust

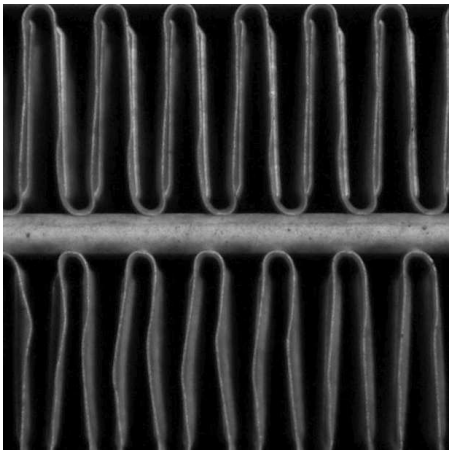

Heat Exchanger B Clean

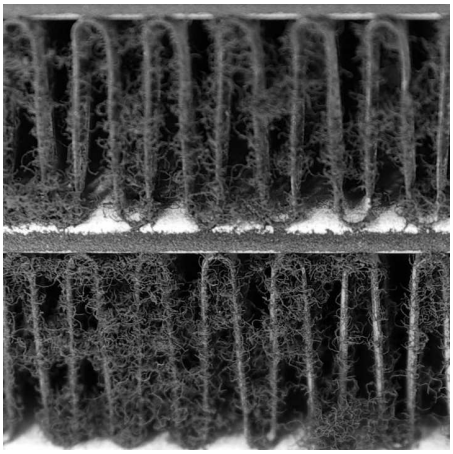

Heat Exchanger B Fouled with 135g ASHRAE Test Dust

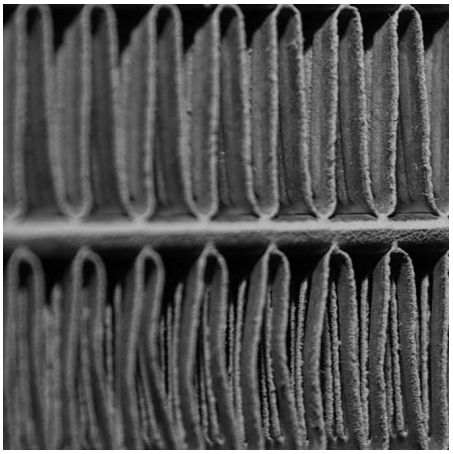

Heat Exchanger B Fouled with 500 g Arizona Road Test Dust

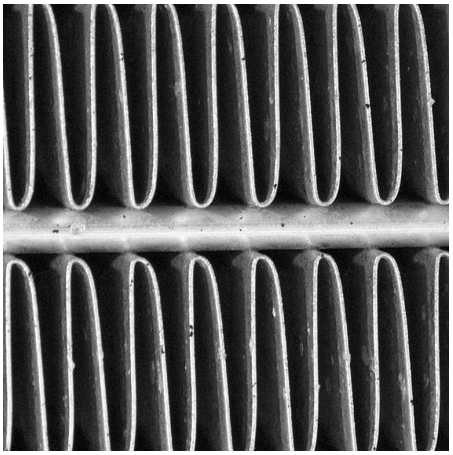

Heat Exchanger C Clean

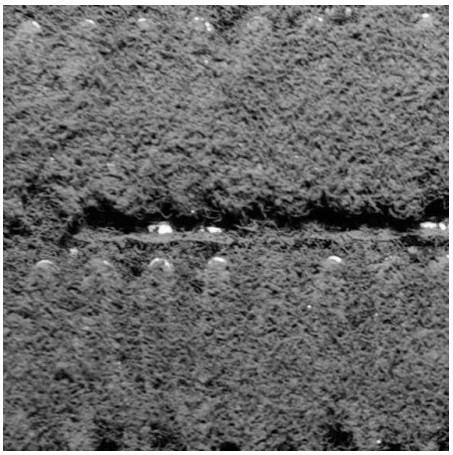

Heat Exchanger C Fouled with 267 g ASHRAE Test Dust

Figure 10: Macro photographs of heat exchangers fouled with dust